will be substantially less than suggested in Figures 2 and 3 and will be much longer ranged in character than the primary–primary transition state interactions. For example,

$$\frac{\gamma_{cc}(3.00\text{ Å})}{\gamma_{cc}(1.75\text{ Å})} = 0.24 \quad \frac{\gamma_{cn}(3.00\text{ Å})}{\gamma_{cn}(1.75\text{ Å})} = 0.18 \quad \frac{\gamma_{co}(3.00\text{ Å})}{\gamma_{co}(1.75\text{ Å})} = 0.14^{2b}$$

(33) The LUMO secondary orbital coefficients are similar in magnitudes in β-phenylmethyl propiolate. However, the secondary orbital coefficients in the next LUMO are large and only the primary–secondary interaction involving the carbomethoxy group will be bonding in the interaction of this MO with the HOMO of the dipole. No reversals are predicted in these cases if only the primary orbital coefficients are considered.
(34) K. Hultzch, *Angew. Chem.*, **60**, 179 (1948).

Monte Carlo Studies on the Structure of a Dilute Aqueous Solution of Methane

S. Swaminathan, S. W. Harrison, and David L. Beveridge*

Contribution from the Chemistry Department, Hunter College of the City University of New York, New York, New York 10021. *Received December 2, 1977*

Abstract: Statistical thermodynamic computer simulations on the dilute aqueous solution of methane at 25 °C under canonical ensemble conditions are reported. The calculations employ the Monte Carlo–Metropolis method based on potential functions representative of ab initio quantum mechanical calculations. Calculated partial molar internal energies and radial distribution functions are presented. The results are analyzed for the statistical state of the system in terms of quasicomponent distribution functions for coordination numbers and binding energies and difference quasicomponent distribution functions. The local solution environment of methane is directly identified with a composite of distorted, defective pentagonal dodecahedral clathrate contributions. The structure of solvent water involves an increase in four-coordinate contributions as compared to pure water.

I. Introduction

The dilute aqueous solution of methane is a system of prominent interest in molecular liquids as the prototype of a nonpolar molecular solute dissolved in liquid water. Moreover, a detailed knowledge of the structure of the methane–water solution at the molecular level can provide leading information on the interaction of water with dissolved hydrocarbon chains in general and thereby contribute to the theoretical basis for understanding the role of water in maintaining the three-dimensional structural integrity of biological macromolecules in solution.

We report herein new theoretical studies of the methane–water intermolecular interaction and Monte Carlo computer simulations of the dilute aqueous solution of methane under canonical ensemble conditions, with temperature T, volume V, and number of particles N specified and constant. All simulations are based on pairwise potential functions representative of ab initio quantum mechanical calculations of the intermolecular interactions.

Our analysis of solution structure is developed in terms of quasicomponent distribution functions in a manner consistent with a previous analysis of liquid water structure contributed from this laboratory. Perturbations of water structure by dissolved methane are developed in terms of difference quasicomponent distribution functions. This study forms an integral part of a series of theoretical investigations on the solvation of prototype biomolecular functional groups and solvent effects on noncovalent biomolecular processes currently underway in this laboratory.

II. Background

General backgrounds on solutions of nonpolar solutes in water have been recently reviewed by Franks[1] and Ben-Naim.[2] Early important work on this system is due to Eley[3] and Frank and Evans.[4] Methane has been identified as a "structure maker" in aqueous solution in the language of Frank and Wen.[5] The nature of structural changes in solvent water by dissolved hydrocarbons has for some time been discussed in terms of water clathrate formation[6] based on work by Glew[7] and analogies drawn from a number of hydrate crystal structures of nonpolar species,[8] known to involve water clathrate cages of order 20 and 24.

Early computer simulations of the methane–water system were reported by Dashevsky and Sarkisov.[9] Recent important theoretical studies of the methane–water system are the ab initio molecular orbital calculations of the methane–water pairwise interaction energy by Ungemach and Schaefer[10] and the Monte Carlo computer simulation on the dilute aqueous solution in the isothermal–isobaric ensemble by Owicki and Scheraga[11] (OS). The OS simulation was based on the water–water potential discussed below and a potential function representative of the Ungemach–Schaefer calculations for the methane–water interaction. Due to limitations in the potential functions, the density of the system in these calculations turned out to be somewhat lower than that observed at 25 °C; still analysis of the results gave the best quantitative theoretical evidence of structuration of vicinal water in the solution to date and the calculated average methane–water coordination number of 23 is consistent with water clathrate contributions to the solution structure.

Theoretical studies of the methane–water solution require an accurate description of the structure of the pure solvent, liquid water, as a point of departure. The structure of liquid water has been the subject of two recent Monte Carlo computer simulations, one from this laboratory using the canonical (T,V,N) ensemble[12] and the other by Owicki and Scheraga in the isothermal–isobaric (T,P,N) ensemble.[13] Both calculations are based on the analytical pairwise potential function for the water–water interactions representative of ab initio quantum mechanical configuration interaction calculations,[14] known to give reasonable agreement with experimental data on the oxygen–oxygen radial distribution function.[15] The calculated radial distribution functions of liquid water are seen to be very sensitive to electron correlation effects in the intermolecular potential function.[12]

The individual papers contain considerable additional details on the structure of water from different but mutually com-

0002-7863/78/1500-5705$01.00/0

plementary viewpoints. The details of our analysis were based directly on Ben-Naim's quasicomponent distribution functions[2] for coordination number and binding energy. The distribution of coordination numbers ranged from 2 to 6 and consisted of some 47% four-coordinate species, with 3, 5, and 6 indicated at the 19, 24, and 6% levels, respectively.[12] Both studies[12,13] are supportive of a unimodal distribution of energetic environments for water molecules in the statistical state of the liquid at 25 °C.

This paper describes the extension of our (T,V,N) ensemble studies on liquid water to the dilute aqueous solution of methane, maintaining the use of potential functions representative of quantum mechanical calculations of the pairwise interaction energies. The analysis of solution structure involves the calculated distribution of coordination numbers and binding energies in the statistical state of the solution and identifies explicitly the supermolecular structures with high statistical weights. Additional theoretical questions we have taken up beyond previous studies include electron correlation effects on the methane-water potential and on solution structure, methane excluded volume effects on solution structure, and quantitative consideration of solute perturbations on solvent structure as quantitatively described by difference quasicomponent distribution functions.

III. Calculations

We consider herein the diffusionally averaged equilibrium structure of the dilute solution of methane in water using the Metropolis method[16] for statistical thermodynamic Monte Carlo computer simulation. The literature of this general type of calculation has recently been reviewed by Barker and Henderson.[17] The specific formulation of the problem and notation relevant to this study are given in our previous paper on liquid water structure. The Monte Carlo calculations involve one methane molecule and 124 water molecules at 25 °C at a density of 1 g/cm^3; this is within 1% of the density computed from the observed partial molar volumes of methane and water.[2] The condensed phase environment is modeled by conventional periodic boundary conditions in the minimum image convention.[18] Standard deviations on each of the quantities calculated are determined using control functions in the manner set forth by Wood.[19]

The configurational energy of the system is developed under the assumption of pairwise additivity of intermolecular interactions using potential functions representative of ab initio quantum mechanical calculations of the water-water and methane-water interaction energies. For the water-water interaction energy we have carried over the potential function developed by Matsuoka, Clementi, and Yoshimine[14] based on moderately large configuration interaction calculations on the water dimer and used in previous studies.[12]

For the methane-water interaction energy, we have recently reported an analytical potential function representative of ab initio 6-31G molecular orbital (MO) calculations[20] using the "Heuristic Potential Function" Method.[21] The final form of the function is determined from interaction energies calculated for 225 methane-water configurations generated by independent random positional and orientational deployments of a water molecule with respect to methane within a center of mass separation of 5.5 Å. The function passes smoothly into the correct limiting behavior of the interaction energy at infinite intermolecular separation. The overall standard deviation of the function is 0.41 kcal/mol and interaction energies within 2 kcal/mol of the minimum, given preferential weighting in the curve fitting procedure, are described within a standard deviation of 0.14 kcal/mol. The predictive value of the function for energies within 2 kcal/mol of the minimum is estimated at $\sigma = 0.30$ kcal/mol. This function is commensurate in quality with the calculations of the methane-water interaction energy by Ungemach and Schaefer,[10] and thus with the potential function used in the OS simulation. The MO function is defined in Table I. The nature of the methane-water interaction as described by the MO function is shown in Figure 1.

Table I. Coefficients a, b, and c of Atomic and Pseudo-Atomic (PSA) Terms in the Methane-Water MO STO 6-31G Intermolecular Potential Function[a]

	inverse power of r	C	H
CH_4	12	1.19×10	4.72×10^{-2}
	1	-9.75×10^{-3}	2.41×10^{-3}
	3	$-9.07 \times 10^{+2}$	$1.93 \times 10^{+2}$

	inverse power of r	O	H	PSA
H_2O	12	$2.88 \times 10^{+5}$	$1.03 \times 10^{+4}$	$-4.12 \times 10^{+4}$
	1	$-1.37 \times 10^{+2}$	1.14×10	3.78
	3	4.98×10^{-3}	1.24×10^{-3}	4.19×10^{-4}

[a] The functional form[b] is

$$V = \sum_{i,j} \left\{ \frac{a_i a_j}{r_{ij}^{12}} + \frac{b_i b_j}{r_{ij}} + \frac{c_i c_j}{r_{ij}^{3}} \right\}$$

$$i \in CH_4; j \in H_2O$$

where r_{ij} is the interatomic separation of atoms (or PSA) i and j. For methane, $r_{CH} = 1.09$ Å and bond angles are tetrahedral. For water, $r_{OH} = 0.957$ Å and ∠HOH is 104.52°. The PSA centers are tetrahedrally coordinated to the oxygen atom at a distance of 0.1852 Å. [b] This function is used for the calculation of interaction energies for intermolecular center of mass separations ≤7.75 Å; energies beyond this point are taken as zero in the spherical cutoff/minimum image convention. This function as it stands would suffer from quasi-ionic effects as $r \to \infty$ and if used without a consistent truncation point could result in N dependence in computer simulation. The problem can be eliminated by curve fitting under the constraint that the coefficients of terms in r^{-n}, $n \leq 3$, balance, as described by Jorgensen and Cournoyer.[28]

The structure of liquid water was previously observed to be quite sensitive to electron correlation effects in the water-water pairwise interaction.[12] The pairwise interaction between methane and water is expected to be relatively weak (ca. $(1\text{-}2)k_BT$) and is also expected to be significantly dependent upon electron correlation. For the purposes of the present study, we have calculated the second-order Moller-Plesset (MP) correlation energy[22] for the methane-water interaction at each of 95 lowest energy points involved in the determination of the STO 6-31G MO function described in the previous paragraph and developed an analytical potential function representative of MP calculations. The MP function is given in Table II. The nature of the methane-water interaction as described by the MP function is shown in Figure 2. The standard deviation of the function is $\sigma = 0.13$ kcal/mol for all points below 2 kcal/mol. A comparison of the MO and MP energies for a slice of the methane-water potential energy hypersurface is given in Figure 3. Electron correlation effects are seen to reduce the binding energy by ~0.5 kcal/mol in low energy regions and decrease the equilibrium methane-water separation by ~15 Å.

Monte Carlo computer simulations are described herein based on each of three functions: The MP function, the MO function, and a related function we call "hard methane" (HM), obtained from the MO function by setting the attractive part of the MO function everywhere to zero in the manner of Barker and Henderson.[23] A comparison of the results of simulations based on the MP and MO potentials gives an idea of the effect of electron correlation on the structure of the solution in a

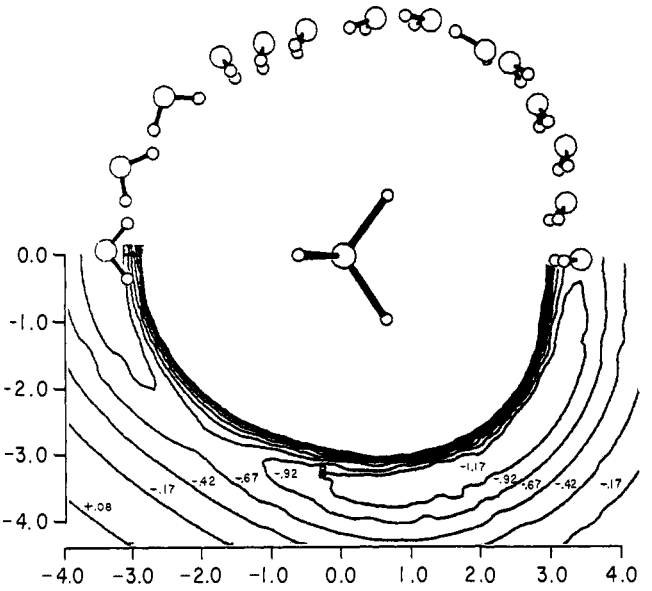

Figure 1. Isoenergy contour map of orientationally optimized methane-water interaction energies calculated from the (12-1-3) STO 6-31G MO potential function for the H-C-H plane. The distance coordinates refer to the separation between the centers of mass of the methane and water molecules in Å. The molecular geometry corresponding to a given energy is depicted in a mirror image position in the top half of the plot. The relative size of the molecules is scaled down to make the plot more legible.

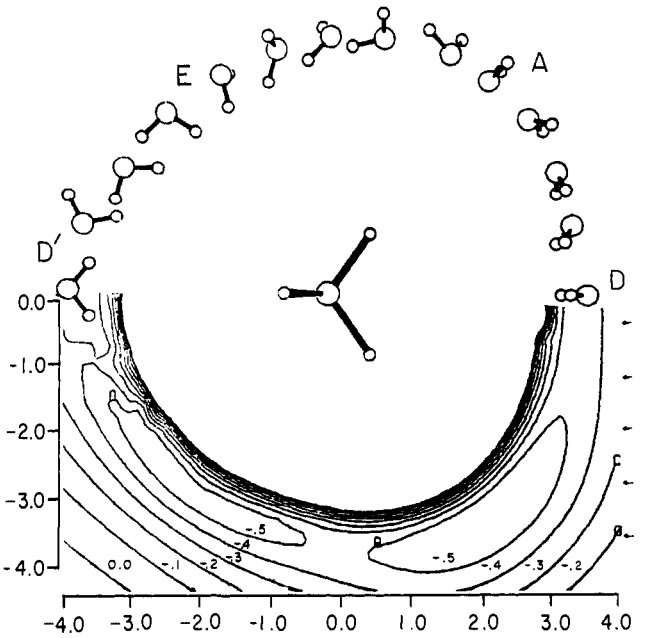

Figure 2. Isoenergy contour map of orientationally optimized methane-water interaction energies calculated from the (12-1-3) MP potential function for the H-C-H plane. See caption to Figure 1 for further details.

Table II. Coefficients *a*, *b*, and *c* of Atomic and Pseudo-Atomic (PSA) Terms in the Methane-Water MP intermolecular Function; see Table I for Definition of Functional Form[a]

	inverse power of *r*	C	H
CH_4	12	-4.07×10^{-1}	-1.61×10^{-2}
	1	-9.78×10^{-3}	2.40×10^{-3}
	3	-1.28×10^{3}	2.05×10^{2}

	inverse power of *r*	O	H	PSA
H_2O	12	-4.38×10^{6}	-2.62×10^{5}	-5.93×10^{5}
	1	-5.65×10^{2}	6.08×10	1.88×10^{2}
	3	1.38×10^{-2}	-8.79×10^{-4}	-4.56×10^{-3}

[a] See footnote *b*, Table I.

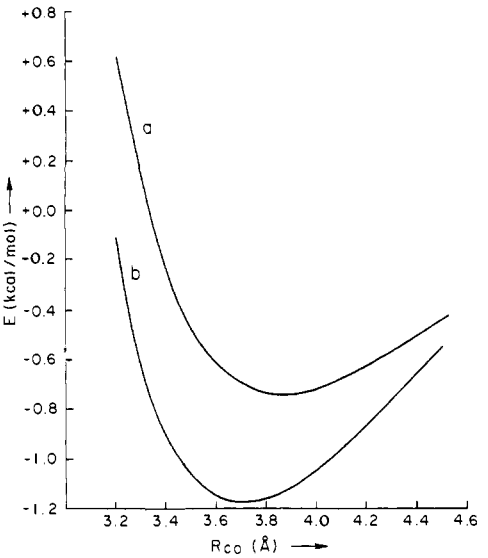

Figure 3. A comparison of the MO (a) and MP (b) energies as a function of distance for geometry A of ref 10 (see also A in Figure 1).

manner analogous to that described previously for liquid water. The structure of the methane-water solution is expected to be largely due to methane excluded volume effects, and a comparison of simulation results based on MP and MO potentials with those obtained from the HM function permits a quantitative study of this particular feature of the system.

The principal point of comparison between calculation and experiment in this work is the thermodynamic partial molar internal energy of transfer $\bar{U}_S$ for solute (S) methane from dilute gas phase to aqueous solution. This and other internal energies relevant to this work are formally defined in Figure 4 and the equations below. Following Ben-Naim, we write the expansion

$$U_{SW}(T,V,N_W,N_S) = U_W(T,V,N_W) + \left(\frac{\partial U}{\partial N_S}\right)_{T,V,N_W} N_S + \ldots \quad (1)$$

where U_{SW} is the total internal energy of N_W water molecules and N_S solute molecules at temperature T and volume V, and U_W is the total internal energy for N_W water molecules. In the addition of one solute molecule to water, $N_S = 1$ and the internal energy of transfer, neglecting higher order terms, is

$$\bar{U}_S = \left(\frac{\partial U}{\partial N_S}\right)_{T,V,N_W} = U_{SW}(T,V,N_W,N_S = 1) - U_W(T,V,N_W) \quad (2)$$

The quantities U_{SW} and U_W are produced directly in computer simulations of the solution and pure solvent respectively as the configurational averages

$$U_{SW}(T,V,N_W,N_S) = \int \ldots \int E(\mathbf{X},^S\mathbf{X}^W) P(\mathbf{X}^S,\mathbf{X}^W)\, d\mathbf{X}^S d\mathbf{X}^W \quad (3)$$

and

$$U_W(T,V,N_W) = \int \ldots \int E(\mathbf{X}^W) P(\mathbf{X}^W)\, d\mathbf{X}^W \quad (4)$$

Table III. Calculated Internal Energies for the Dilute Aqueous Solution of Methane at 25 °C Based on the MP, MO, and HM Potential Functions in kcal/mol

	MP	MO	HM
U_{SW} (N_W = 124, N_S = 1)	−1077.7 ± 3.6	−1076.2 ± 3.6	−1070.1 ± 3.6
U_W (N_W = 124)	−1054.4 ± 5.5	−1054.4 ± 5.5	−1054.4 ± 5.5
$U_{W'}$ (N_W = 124)	−1079.4 ± 3.6	−1077.9 ± 3.6	−1075.3 ± 3.6
$\bar{U}_{S'}$	1.71 ± 0.29	1.73 ± 0.27	5.19 ± 0.27
$\bar{U}_{rel}$	−25.0 ± 6.6	−23.5 ± 6.6	−20.9 ± 6.6
$\bar{U}_S$	−23.3 ± 6.6	−21.8 ± 6.6	−15.7 ± 6.6

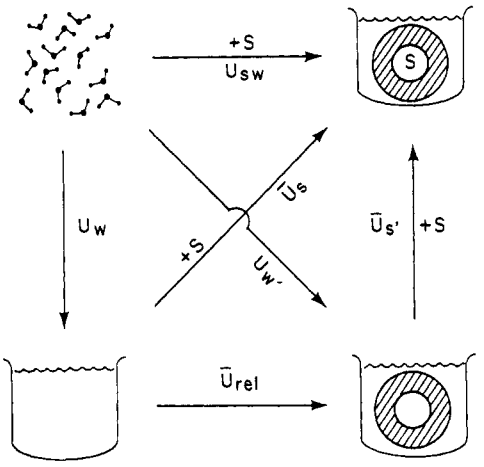

Figure 4. Thermocycle illustrating the energetic quantities produced in a Monte Carlo computer simulation of a dilute solution of solute, S, in water, W.

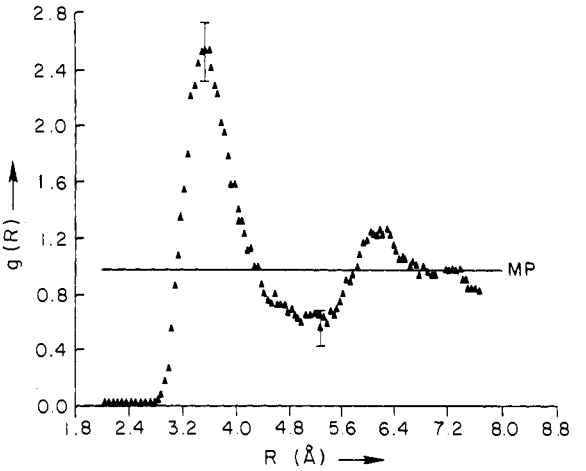

Figure 5. Calculated methane–water radial distribution function $g(R)$ vs. center of mass separation R from Monte Carlo computer simulation based on the MP function.

where $E(\mathbf{X}^S,\mathbf{X}^W)$ is the configurational energy of the system with solute specified by the configurational coordinates $\mathbf{X}^S$ and the N_W solvent water molecules specified by the configurational coordinates $\mathbf{X}^W$. The quantity $P(\mathbf{X}^S,\mathbf{X}^W)$ is the probability of observing the system in configuration $\{\mathbf{X}^S,\mathbf{X}^W\}$. The quantities $E(\mathbf{X}^W)$ and $P(\mathbf{X}^W)$ are analogous terms for pure water. Thermodynamic quantities expressed on a per particle basis are notated by a bar, as in $\bar{U}_S$.

Reference to Figure 4 shows an alternative formulation of $\bar{U}_S$ to be

$$\bar{U}_S = \bar{U}_{S'} + \bar{U}_{rel} \tag{5}$$

The definition of the quantities on the right hand side of eq 5 follows from partitioning the configurational energy according to

$$E(\mathbf{X}^S,\mathbf{X}^W) = E_{SW}(\mathbf{X}^S,\mathbf{X}^W) + E_{WW}(\mathbf{X}^W) \tag{6}$$

where E_{SW} and E_{WW} are solute-water and solvent water contributions, respectively, defined under the assumption of pairwise additivity as

$$E_{SW}(\mathbf{X}^S,\mathbf{X}^W) = \sum_i^{N_W} E_i(\mathbf{X}^S,\mathbf{X}_i{}^W) \tag{7}$$

and

$$E_{WW}(\mathbf{X}^W) = \sum_{i<j}^{N_W} E_{ij}(\mathbf{X}_i{}^W,\mathbf{X}_j{}^W) \tag{8}$$

where E_i and E_{ij} are solute-water and water-water pairwise interaction energies. The transfer quantity $\bar{U}_{S'}$ is then defined as

$$\bar{U}_{S'} = \int \dots \int E_{SW}(\mathbf{X}^S,\mathbf{X}^W) P(\mathbf{X}^S,\mathbf{X}^W)\, d\mathbf{X}^S d\mathbf{X}^W \tag{9}$$

and represents the direct solute-solvent contribution to the partial molar internal energy of transfer. The quantity $\bar{U}_{S'}$ can be written in terms of the quasicomponent distribution function for solute binding energy

$$\bar{U}_{S'} = \int_{-\infty}^{+\infty} \nu x_B(\nu)\, d\nu \tag{10}$$

where $x_B(\nu)$ is mole fraction of methane molecules with binding energy ν. The second term on the right hand side of eq 5 represents a contribution from solvent reorganization on solution formation and hence can be expressed in terms of a difference of a pure water term U_W and a solvent water term $U_{W'}$

$$\bar{U}_{rel} = U_W - U_{W'} \tag{11}$$

where

$$U_{W'} = \int \dots \int E_{WW}(\mathbf{X}^W) P(\mathbf{X}^S,\mathbf{X}^W)\, d\mathbf{X}^S d\mathbf{X}^W \tag{12}$$

Note $\bar{U}_{rel}$ is defined per solute particle.

IV. Results

The simulation using the MP potential is based on a 750K stochastic walk, with the first 100K discarded in forming the ensemble averages. Convergence criteria and error bounds were determined from control functions taken at 25K intervals in the calculations. The number of discards was determined from minimum error bounds. The partial molar internal energy of methane is −23.3 ± 6.6 kcal/mol, compared with an experimental value of −2.6 kcal/mol.[24] The complete set of calculated energetic quantities for all simulations reported are collected in Table III.

The calculated radial distribution function for the center of mass of water molecules with respect to the center of mass of the methane molecule for the MP function is shown in Figure 5. We find a broad unstructured first peak and a minimum in the region of 5.3 Å. Integrating $g(R)$ up to this point yields an average water coordination number of 19.35. Experimental values for these quantities are not known, but taking

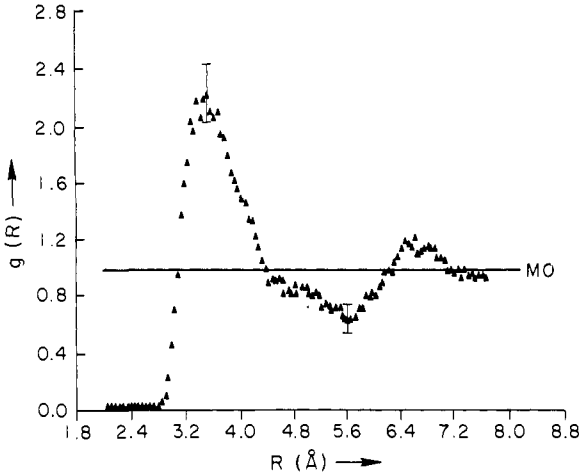

Figure 6. Calculated methane–water radial distribution function $g(R)$ vs. center of mass separation R from Monte Carlo computer simulation based on the MO function.

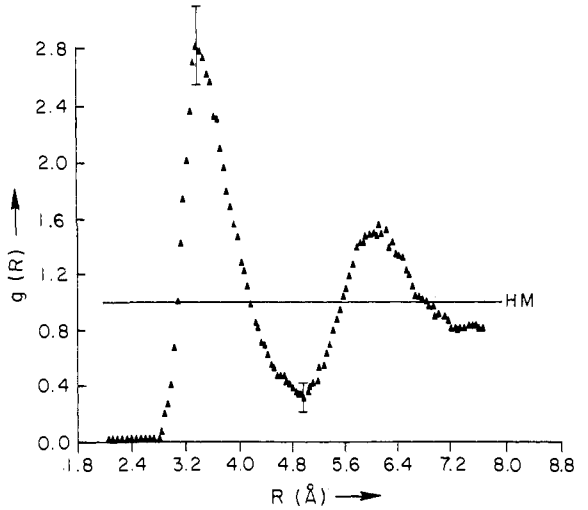

Figure 7. Calculated methane-water radial distribution function $g(R)$ vs. center of mass separation R from Monte Carlo computer simulation based on the HM function.

into account differences in the (T,V,N) and (T,P,N) ensembles we find them in satisfactory accord with the calculated results of Owicki and Scheraga.

The simulation involving the MO potential function was based on 575K steps with 150K discarded. The calculated partial molar internal energy for methane was found to be -21.8 ± 6.6 kcal/mol. The calculated methane-water radial distribution function is given in Figure 6.

The simulation on hard methane involved 900K steps with 275K discarded. The calculated partial molar internal energy was -15.7 ± 6.6 kcal/mol. The radial distribution function calculated with the HM potential function is given in Figure 7.

A theoretical analysis of the structure of the dilute aqueous solution of methane can be developed in terms of quasicomponent distribution functions for coordination number and binding energies defined as described by Ben-Naim in ref 2. The distribution of coordination numbers found within the first hydration shell ($R_M = 5.3$) of methane in the statistical state of the solution is shown for all three simulations in Figure 8. Here we plot the mole fraction of particles $x_C(K)$ vs. coordination number K in histograph form. The $x_C(K)$ from the MP simulation is a broad unimodal distribution ranging from $K = 16$ to 22 with a maximum in the region of $K = 19$ and 20,

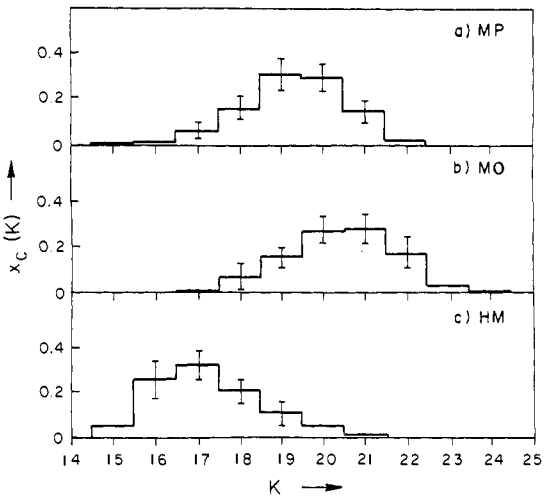

Figure 8. Calculated quasicomponent distribution function $x_C(K)$ vs. coordination number K for (a) the MP function, (b) the MO function, and (c) the HM function.

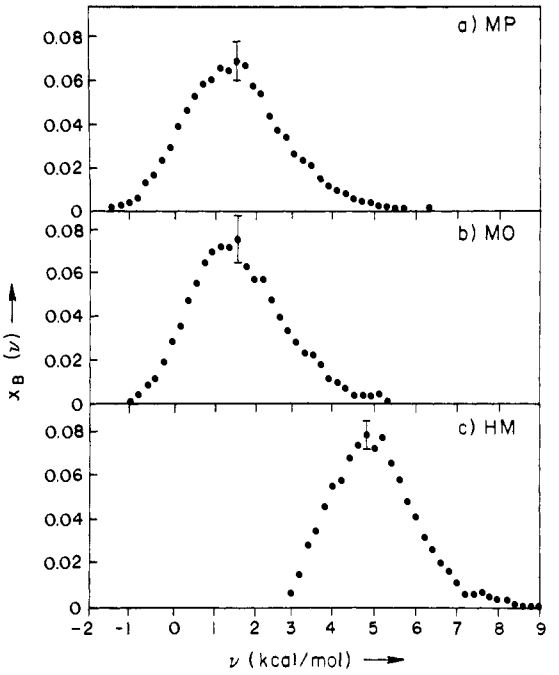

Figure 9. Calculated quasicomponent distribution function $x_B(\nu)$ vs. binding energy ν for (a) the MP function, (b) the MO function, and (c) the HM function.

biased slightly in shape toward higher coordination numbers. The $x_C(K)$ for the MO simulation is slightly more symmetric, and the maximum is displaced to the region of $K = 17$ and 18. The HM simulation produces a slightly broader distribution of coordination numbers, unimodal with a maximum at $K = 17$ and clearly biased toward higher K.

The calculated quasicomponent distribution functions for binding energy, the mole fraction of particles $x_B(\nu)$ as a function of methane binding energy in the system, is shown for all three simulations in Figure 9. All $x_B(\nu)$ distributions are of a similar shape but displaced toward higher energy on going from the results of the MP simulation to those obtained from the HM potential. There is some incipient structure in the curve but the error bounds on the calculated values are too large to ascribe any statistical significance.

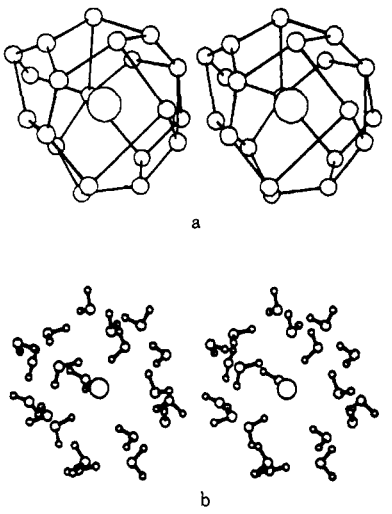

Figure 10. Stereographic view of methane and its first hydration shell taken from a structure with high statistical weight in $x_C(20)$ of the MP simulation. (a) Disposition of centers of mass of water molecules about methane (shaded) with the quasiclathrate cage delineated; (b) disposition of water molecules about methane in the structure. Relative sizes of molecules scaled down for greater legibility in the figure; methane represented as a sphere.

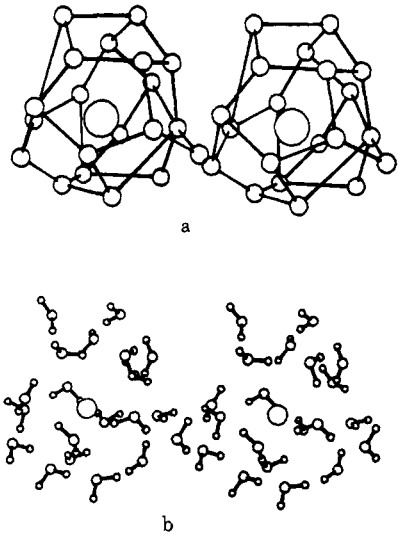

Figure 11. Stereographic view of methane and its first hydration shell taken from another structure with high statistical weight in $x_C(20)$ of the MP function. (a) Disposition of centers of mass of water molecules about methane (shaded) with the quasiclathrate cage delineated; (b) disposition of water molecules about methane in the structure.

V. Discussion

This section deals with the following problems: (a) the comparison of calculated and observed partial molar internal energies for methane in aqueous solution, (b) the microscopic nature of the local solution environment of the solute methane, (c) electron correlation effects on solution structure, (d) the role of the soft part of the methane-water potential on solution structure, and (e) structuration effects in solvent water due to solute methane.

Comparing the calculated and observed partial molar internal energies for methane in water, the calculated values from each of the three simulations, MP, MO, and HM, are seen to be negative but rather too low. The negative sign on this term is an essential feature of the hydrophobic effect as currently understood and has been ascribed to solvent water stabilization effects. The partitioning of $\overline{U}_S$ into solute effect $\overline{U}_{S'}$ and a solvent relaxation contribution $\overline{U}_{rel}$ is displayed in Table III. The $\overline{U}_{S'}$ contribution is positive for all simulations and $\overline{U}_{rel}$ is negative, consistent with current ideas on the hydrophobic effect. The solvent stabilization term is somewhat overestimated, however, and leads to a factor of 10 discrepancy between calculated and observed $\overline{U}_S$ values, a difference of the order of 20 kcal/mol. If we assume this stabilization involves mainly those ~20 water molecules found in the first hydration shell of methane, this is an error of 1 kcal/mol per water molecule or a fraction of a kcal/mol per pairwise interaction or hydrogen bond. The major assumptions inherent in the calculations are the neglect of three-body and higher order contributions to the configurational energy, truncation errors in the quantum mechanical calculations of the pairwise interaction energies, and statistical errors in the analytical potential function. The discrepancy between calculated and observed values is thus reasonable in perspective of the capabilities and limitations of the configurational energy evaluation.

The distribution of coordination numbers for methane in the statistical state of the dilute aqueous solution of methane is consistent with water clathrate contributions. Our values are closer to those expected for a pentagonal dodecahedral cage whereas the corresponding results obtained in the OS (T,P,N) simulation were closer to the coordination number expected for the tetrakaidecahedral cage. In order to investigate further the microscopic nature of the local solution environment of methane, we have extracted a number of low energy configurations from $x_C(19)$ and $x_C(20)$ quasicomponents in the MP simulation and made stereographic ORTEP[25] plots of methane and its first hydration shell. The structure which most closely resembles pentagonal dodecahedral clathrate cage is given in Figure 10. The resemblance seems to provide direct confirmation of clathrate contribution to the solution structure. In a number of the other structures the clathrate-like regions of the first hydration shell could be found but defects and distortions were more prevalent than in Figure 10. We have chosen one such structure that we feel is representative of the sample set and present it in Figure 11. The quasicomponent distribution functions for binding energy $x_B(\nu)$ collected in Figure 9 show that the solute methane is presented with a continuous distribution of energetic environments in the solution. The emergent description of the dilute aqueous solution of methane is that of a slightly distorted and defective continuum clathrate structure.

A comparison of the computer simulation results based on the MP and MO potentials for the methane-water interaction gives an idea of the effects of electron correlation of the system. This may be taken only as leading information, since there are still deficiencies in the quality of points in the quantum mechanical data base due to basis set truncation effects and the nature of Moller-Plesset electron correlation. The calculated $g(R)$ for the MP potential in Figure 5 and the MO potential in Figure 6 are similar in overall appearance with only minor visible discrepancies. The analysis of structure in terms of $x_C(K)$ and $x_B(\nu)$ shows electron correlation discernibly displacing the distribution of coordination numbers to higher values and the distribution of binding energies to lower values. The displacements are of the order of 5-10% in both quantities.

Further comparison of the results with reference to $g(R)$, $x_C(K)$, and $x_B(\nu)$ obtained from the computer simulation based on hard methane provides information on the role of the soft part of the methane-water potential function on solution structure. First, the similarity in the calculated radial distribution functions in Figures 5-7 shows the essential nature of the methane-water solution as an excluded volume effect as expected. The analysis of the structure shows that the soft part of the potential function shifts the distribution of coordination

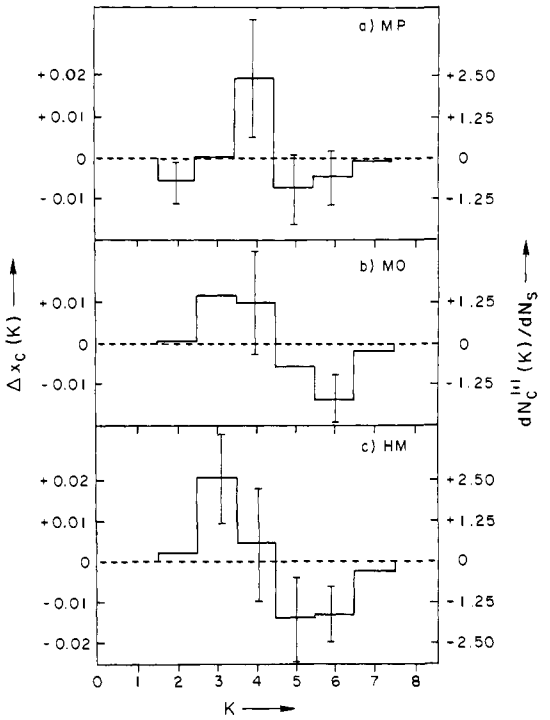

Figure 12. Difference quasicomponent distribution functions $\Delta x_C(K)$ vs. coordination number K for (a) the MP function, (b) the MO functions, (c) the HM function.

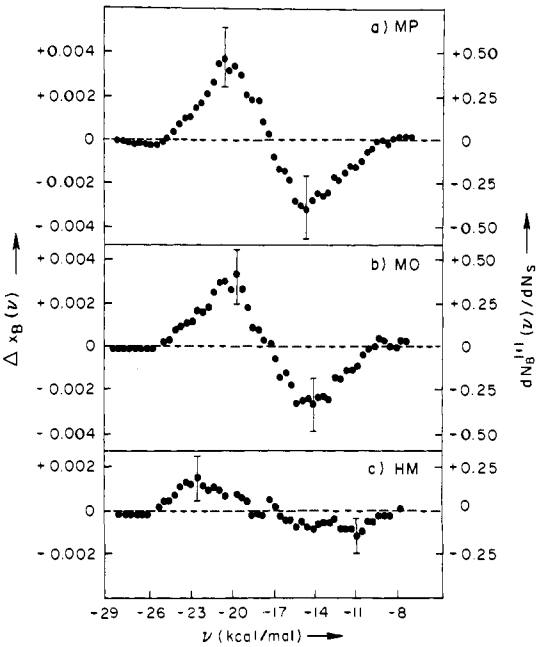

Figure 13. Difference quasicomponent distribution functions $\Delta x_B(\nu)$ vs. binding energy ν for (a) the MP function, (b) the MO function, and (c) the HM function.

numbers upwards by 15% and shifts the distribution of methane-water binding energies down by 3.2 kcal/mol.

Finally we consider the effects of solute methane on water structure. We note that Owicki and Scheraga[11] have identified structuration effects in the solvent by studying explicitly the waters vicinal to the solute by a method involving partitioning of configuration space. A similar analysis is being employed in a molecular dynamics study of a solution of dipeptide in water by Rossky and Karplus.[26] We develop our representation of the phenomenon in terms of difference (Δ) quasicomponent distribution functions. The idea here is to describe the changes in water structure in terms of difference between $x_C(K)$ and $x_B(\nu)$ calculated for the solution and for the pure liquid. The effects of bulk water are removed by the differencing, allowing the direct display of structural changes in solution water without recourse to partitionings of configuration space. The formal significance of difference quasicomponent distribution functions is developed in Appendix A to this paper.

The $\Delta x_C(K)$ and $\Delta x_B(\nu)$ for solvent water in the dilute aqueous solution of methane with respect to bulk water as described in ref 8 are given in Figures 12 and 13. In the distribution of $x_C(K)$ there is a clear increase in four-coordinate species at the expense of coordination numbers K = 2, 5, and 6. These results must be considered in the perspective of the relatively large error bounds on the Δ-QCDF, but the increase in four-coordinate structures is definitely statistically significant. The $\Delta x_B(\nu)$ show slight but clearly discernible shifts toward stronger binding among solvent water molecules. The nature of the solvent structuration with respect to clathrate water molecules as seen from Figures 9 and 10 involves predominantly bent hydrogen bonds rather than linear hydrogen bonds characteristic of ice I.

If one permits the identification of an increase in four-coordinate species in the solvent and increased binding with "structure making", the Δ-QCDF description of structuration effects serves to quantify some of the long standing terminology prevalent in the descriptive chemistry of solutions. The problems inherent in this connection are brought out in the critical review of the problem by Holzer and Emerson,[27] and we reserve judgement on this point until we have determined $\Delta x_C(K)$ and $\Delta x_B(\nu)$ for solvent water in a number of solutions of putative structure makers and structure breakers. We presently have studies parallel to this underway on dilute aqueous solutions of monatomic cations and anions to gain additional insight into this aspect of the problem.

VI. Summary and Conclusions

Monte Carlo computer simulation on the dilute aqueous solution of methane at 25 °C using quantum mechanical potential functions reveals the local solution environment to be that of a distorted defective continuum pentagonal dodecahedral clathrate structure. Increased four coordination and stronger binding is induced in the solvent water as compared with the bulk liquid. Using difference quasicomponent distribution functions to quantify structural perturbations in the solvent, we find increased four coordination and stronger binding in the water as compared to bulk liquid.

Acknowledgment. This research is submitted by S.S. in partial fulfillment of the requirements for the Ph.D. in Chemistry at the City University of New York. Support for this research comes from NIH Grant No. 1-R01-NS12149-03 from the National Institutes of Neurological and Communicative Diseases and Stroke and a CUNY Faculty Research Award. D.L.B. acknowledges U.S.P.H.S. Research Career Development Award 6TK04-GM21281 from the National Institute of General Medical Studies. Helpful discussions with Dr. Rosemary Whitehead and Dr. Mihaly Mezei are gratefully acknowledged.

Appendix A. Difference Quasicomponent Distribution Functions

We present herein considerations on describing perturbations on water structure due to the addition of a solute molecule. The structure of water in an aqueous solution can be defined in terms of quasicomponent distribution functions for coordination number K and binding energy ν as

$$x_C(K) = N_C^{(1)}(K)/N \qquad \text{(A1)}$$

$$x_B(\nu) = N_B^{(1)}(\nu)/N \quad \text{(A2)}$$

Here x_i is the mole fraction of particles in the system with characteristic i, $N_i^{(1)}$ is the first-order quasicomponent distribution function, and N is the number of water molecules in the system. In a solution problem, we wish particularly to determine the quantities such as

$$\frac{dN_C^{(1)}}{dN_S} \text{ and } \frac{dN_B^{(1)}(\nu)}{dN_S} \quad \text{(A3)}$$

the change $dN_i^{(1)}$ in the first-order quasicomponent distribution function with respect to the change in the number of solute molecules dN_S.

Taking coordination number as an example and developing the derivative in terms of finite differences, we have

$$\frac{dN_C^{(1)}(K)}{dN_S} \cong \frac{\Delta N_C^{(1)}(K)}{\Delta N_S} = \Delta N_C^{(1)}(K) \quad \text{(A4)}$$

where ΔN_S has been assigned the value of unity since our system involves the addition of only one solute particle. Now for calculations based on N_W water molecules in the pure liquid and N solvent waters in the solution,

$$\Delta N_C^{(1)}(K) = N_C^{(1)}(K) - N_C^{(1)}(K)^W = Nx_C(K(- N_W x_C(K)^W \quad \text{(A5)}$$

where $x_C(K)$ is the mole fraction of water molecules as a function of K for solvent water in a solution and $x_C(K)^W$ is the corresponding quantity for pure water. In our treatment of the problem, the number of solvent waters N is equal to $N_W - 1$, one of the waters having been replaced by the solute. Using this relationship for N, expanding eq B5, and substituting back into eq B4, we have

$$dN_C^{(1)}(K)/dN_S = N_W \Delta x_C(K) \qquad N_W \gg 1 \quad \text{(A6)}$$

where $\Delta x_C(K)$ is the difference quantity

$$\Delta x_C(K) = x_C(K) - x_C(K)^W \quad \text{(A7)}$$

Analogously for binding energy,

$$dN_B^{(1)}(\nu)/dN_S \simeq N_W \Delta x_B(\nu) \qquad N_W \gg 1 \quad \text{(A8)}$$

where

$$\Delta x_B(\nu) = x_B(\nu) - x_B(\nu)^W \quad \text{(A9)}$$

Note that $\Delta x_C(K)$ alone is a quantity dependent on the number of particles in the system whereas the difference quasicomponent distribution functions $dN_C^{(1)}/dN_S$ and $dN_B^{(1)}/dN_S$ are effectively independent of the number of particles in the system and can be used for absolute comparison among systems.

References and Notes

(1) F. Franks in "Water—A Comprehensive Treatise", Vol. II, F. Franks, Ed., Plenum Press, New York, N.Y., 1972, p 1.
(2) A. Ben-Naim, "Water and Aqueous Solutions", Plenum Press, New York, N.Y., 1974.
(3) D. D. Eley, *Trans. Faraday Soc.*, **35**, 1281 (1939).
(4) H. S. Frank and M. W. Evans, *J. Chem. Phys.*, **13**, 507 (1945).
(5) H. S. Frank and W. Y. Wen, *Discuss. Faraday Soc.*, **24**, 133 (1957).
(6) C. Tanford, "The Hydrophobic Effect", Wiley, New York, N.Y., 1973.
(7) D. N. Glew, *J. Phys. Chem.*, **66**, 605 (1962).
(8) D. W. Davidson, ref 1, p 115.
(9) V. G. Dashevsky and G. N. Sarkisov, *Mol. Phys.*, **27**, 1271 (1974).
(10) S. R. Ungemach and H. F. Schaefer III, *J. Am. Chem. Soc.*, **96**, 7898 (1974).
(11) J. C. Owicki and H. A. Scheraga, *J. Am. Chem. Soc.*, **99**, 7403 (1977).
(12) S. Swaminathan and D. L. Beveridge, *J. Am. Chem. Soc.*, **99**, 8392 (1977).
(13) J. C. Owicki and H. A. Scheraga, *J. Am. Chem. Soc.*, **99**, 7413 (1977).
(14) O. Matsuoka, E. Clementi, and M. Yoshimine, *J. Chem. Phys.*, **64**, 1351 (1976).
(15) G. C. Lie, E. Clementi, and M. Yoshimine, *J. Chem. Phys.*, **64**, 2314 (1976).
(16) N. Metropolis, A. W. Rosenbluth, M. N., Rosenbluth, A. H. Teller, and E. Teller, *J. Chem. Phys.*, **21**, 2087 (1953).
(17) J. A. Barker and D. Henderson, *Rev. Mod. Phys.*, **48**, 587 (1976).
(18) F. Kohler, "The Liquid State", Crane Russack Co., 1972, Chapter 3.
(19) W. W. Wood, in "Physics of Simple Liquids", H. N. V. Temperley, J. S. Rowlinson, and G. S. Rushbrooke, Ed., Wiley, New York, N.Y., 1968, Chapter 5.
(20) W. J. Hehre, R. Ditchfield, and J. A. Pople, *J. Chem. Phys.*, **56**, 2257 (1972).
(21) S. W. Harrison, S. Swaminathan, and D. L. Beveridge, *Int. J. Quantum Chem.*, to be published.
(22) C. Moller and M. S. Plesset, *Phys. Rev.*, **46**, 618 (1934).
(23) J. A. Barker and D. Henderson, *J. Chem. Phys.*, **47**, 2856 (1967); *Acc. Chem. Res.*, **4**, 303 (1971).
(24) M. Yaacobi and A. Ben-Naim, *J. Phys. Chem.*, **78**, 175 (1974); H. Edelhoch and J. C. Osborne, Jr., *Adv. Protein Chem.*, **30**, 188 (1976).
(25) C. K. Johnson "ORTEP: A Fortran Thermal-Ellipsoid Plot Program", ORNL No. 3794.
(26) P. Rossky and M. Karplus, private communication, manuscript in preparation.
(27) A. Holzer and M. F. Emerson, *J. Phys. Chem.*, **73**, 26 (1969).
(28) W. L. Jorgensen and M. E. Cournoyer, *J. Am. Chem. Soc.*, submitted.